Post-print of: Abramski M., Mieloszyk E., Milewska A.: Analysis of compressive forces in CFGFT cylindrical pillars and their coatings using laboratory tests and metric spaces. MEASUREMENT. Vol. 142 (2019), pp. 113-121. DOI: 10.1016/j.measurement.2019.04.056

Analysis of compressive forces in CFGFT cylindrical pillars and their coatings using laboratory tests and metric spaces

M. Abramski, E. Mieloszyk, A. Milewska

Summary

The article discusses compressive forces tests in composite - concrete pillars with the use of laboratory active experiment including the factors and properties of materials which have a significant impact on the test results and their repeatability. A polymer composite based on glass fiber reinforced resin with different fiber beam angles (20°, 55° and 85°) was used as a buffer / coat of the pole. Due to the problems with direct comparison of the obtained discrete measurement results for different angles of the fiber winding, a transition from the measured discrete signals to the continuous description was proposed. Using this approach, it was possible to include control systems, identification theory and finally metric spaces in the research methodology. The latter made it possible to determine the relations between compressive forces for the various examined poles and their coats, and further, to define the partial order in the space of the poles studied and their coverings. The obtained results indicated the wide possibilities of the proposed test methods for compressive forces in composite - concrete pillars and their glass-fiber reinforced coats.

Keywords: composite pillar coating; compressive forces; model identification

1. Introduction

Aerospace, automotive, construction and shipbuilding industries use composite which inevitably undergo physical, chemical and mechanical degradation processes [1]. It is crucial when such materials constitute elements of air, sea or civil structures, whose failure may lead to health hazard or human life threat. The assessment of material structure degradation is related to the detection of irregularities affecting the mechanical properties of a given object and determination of its strength.

Composite materials produced on the basis of resins with reinforcement in the form of carbon fibers (Carbon Fiber Reinforced Polymer, CFRP) or glass fibers (Glass Fiber Reinforced Polymer, GFRP - [2]) are exposed to various damages arising during their operation. Typical types of damage that composite materials undergo include fatigue cracks in the matrix, reinforcement fibers, fiber and matrix delamination (debonding), and in the case of multilayer materials, they also include delamination. These delaminations are often not visible from the outside, so the following methods can be used to detect them: electromechanical impedance, vibration, propagation of elastic waves (these waves are strongly suppressed in composite materials) and terahertz spectroscopy. These methods are also used to test the reliability of composite structures or their components using optical fiber sensors [3].

Delamination can be modeled by separating the beam into subdivisions and introducing additional boundary conditions at their ends [4]. However, the most common method of modeling delamination is the reduction of elastic properties of the material in the area where the stress-related criteria for damage were exceeded [4], [5].

Composite materials, especially those used in construction or aviation during operation, may be exposed to high temperatures, for example a lightning strike. It causes their physical, chemical and mechanical degradation. For example, glass fibers type E, i.e. made of boron-aluminum-silicon glass, also called non-alkaline, have a softening point of about 750°C.

Another important feature of these fibers from the point of view of the construction of composite-concrete pillars considered in the work is their sensitivity to water. The influence of moisture on the decrease of tensile strength is shown in Fig. 1.

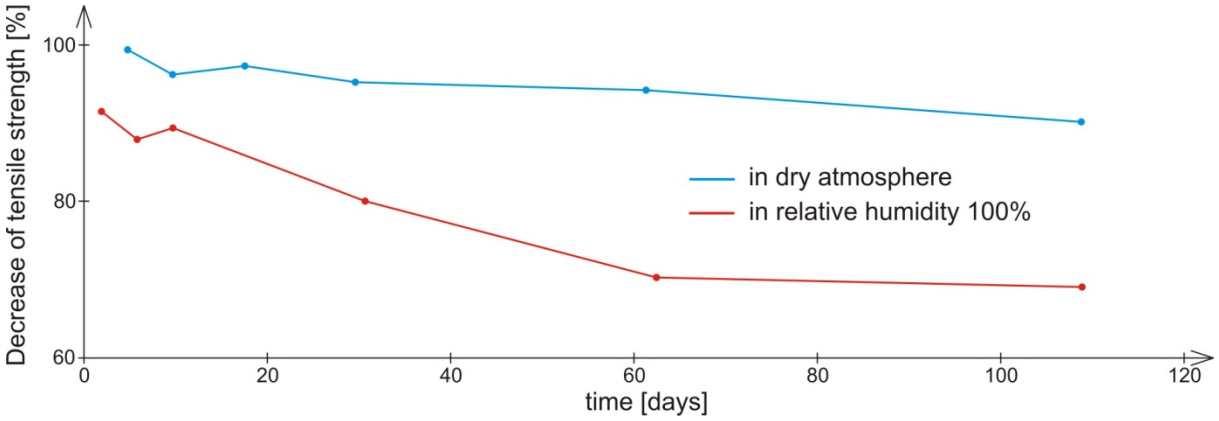

Fig. 1. Drop in tensile strength of glass fibers E during storage in various humidity conditions (Prepared on the basis of literature, including the use of [6])

The basic mechanical property of concrete is its compressive strength. This durability depends on many factors, and above all on the grain size and quality of the aggregate, the quantity and quality of cement and water, as well as the concrete mix production technology, concrete curing conditions in the construction and the age of concrete [7]. Concrete begins to bind after about 1.5 hours after adding water to the dry mix at 20° C. The humidity of the environment in which the concrete is located increases the concrete strength after 28 days of hardening. If the environment is humid, then the strength increases systematically over time and after a dozen or so years it can be much greater than its strength after 28 days. In a dry environment, after about a year, the concrete strength increases by approximately 40% compared to the strength after 28 days and then remains practically unchanged or slightly reduced.

From these materials (concrete, composite), it is possible to construct cylindrical pillars with different heights and diameters of 2r. These are CFGFT (Concrete Filled Glass Fiber-Reinforced Polymer Tube) columns, i.e. poles in the form of a concrete filled tube made of polymer composite reinforced with glass fibers. The composite tube will be called a buffer or a pole coat. It is obvious that a pole constructed in this way has mechanical and strength features from concrete as well as from the composite and its reinforcements. This combination of materials creates new construction and operating possibilities for pillars. Therefore, tests of this

type of columns will be presented in the further part of the work in contrast to the research concerning columns in the steel coating [8] or composite coating, but reinforced with fibers only in circumferential direction [9]. The facts presented earlier were the guiding idea for planning an active experiment, preparing materials for experimental (laboratory) research, methodology for conducting experiments, registration of research results and their description. Everything was also prepared in terms of the possibility of mathematical approach to the problem in the form which was not used before in the source literature for an analyzing the presented problems.

2. Materials for experimental / laboratory research and their properties

A batch of CFGFT cylindrical pillars with a height of h = 200 cm was prepared for the tests. The column coat was made of a polyester resin tube. The tube was made using a continuous winding method and reinforced with continuous glass fibers. E-type glass fibers used in the production of tubes were in the form of continuous roving with a linear density of 2400 g/m. Tubes with different beam angles of continuous glass fiber bundles were prepared - Fig. 2. These were 20°, 55° and 85° angles, and the beam was cross-shaped.

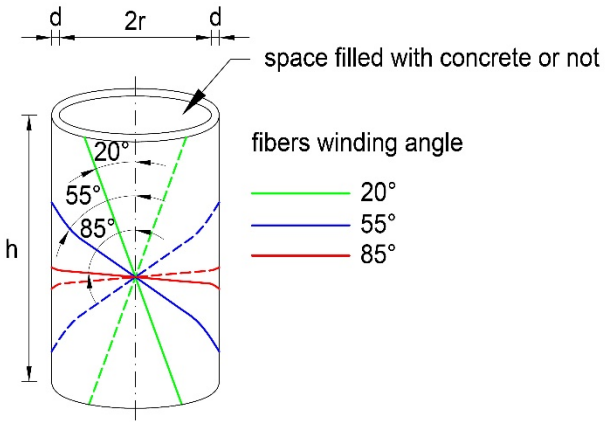

Fig. 2. Scheme of the buffer / coat cover with the beam angles of the glass fibers marked.

In each case, the fiber content declared by the manufacturer was 60%. The actual content of fibers in the composite was verified by the standard method [10] used, among others in the US. The test was carried out in a Womach furnace with a temperature range up to 1300°C, with the furnace being heated in accordance with [10] to a temperature of 535°C. The samples of the reinforced composite used for this study were obtained randomly from each type of pillar by cutting rectangles with sides of 25 mm and 30 mm, respectively. The weight of the samples ranged from 8.0 g to 10.2 g. The weight used for the measurements was characterized by the measurement accuracy 0.0001 g. The results obtained from the measurements are shown in Table 1.

Table 1. Fiberglass content in the sample.

	For a tube with a beam angle of glass fibers		
	20º	55º	85º
Average proportion of glass fibers in the sample mass $\bar{f}_g$ [%]	69,3	58,4	72,4
Mean square deviation is s^2 from the average sample weight [%]^2	2,28	0,59	0,22
s [%]	1,51	0,77	0,47
Average proportion of glass fibers in the sample volume $\bar{f}_v$ [%]	49,1	37,5	52,8

The volume content of fibers in the composite given in Table 1 was determined based on the theory of composites [11], according to the formula

$$\bar{f}_v = \frac{\rho_m \bar{f}_g}{\rho_m \bar{f}_g + (100 - \bar{f}_g)\rho_l} \quad (1)$$

where ρ_m and ρ_l are the densities of the resin matrix and reinforcement fibers, respectively. Their values based on [11] were assumed as 1.1 g/cm^3 and 2.58 g/cm^3 respectively. The remaining symbols used in the formula are defined in Table 1.

In addition, thanks to these tests, by analyzing the macroscopic system of fibers remaining after firing the resin, the information about eleven layers of roving was obtained The producer reported that a single layer of roving is formed after eight passes, and one roving band has a width of 7 to 8 cm.

The inner diameter 2r declared by the pipe manufacturer was 200 mm, and the thickness d of the wall was to be between 5,5 and 6,0 mm. The first of these quantities corresponded exactly to reality, while the wall average thickness ranged from 5,8 to 7,1 mm. This was established on the basis of measurements of the thickness of the composite pipe wall samples. The measurements were carried out using a Vernier caliper on 25 mm wide rims of the tubes. For each of the three series of tubes, six such rims were prepared. Wall thickness measurement was performed for each rim in eight places, evenly distributed around the perimeter of the rim every 45°. Table 2 presents the information resulting from the measurements carried out on the wall thickness of the tubes. This results in a large heterogeneity of the parameter d.

Table 2. The results of tube wall thickness measurement.

	For a tube with a beam angle of glass fibers		
	20º	55º	85º
Average wall thickness [mm]	7,1	6,5	5,8
Average square deviation s^2 from the average wall thickness $[mm]^2$	0,5	0,4	0,01
s $[mm]$	0,7	0,6	0,1
Range [mm]	3,1	3,0	0,5

The preparation of CFGFT columns (h = 200cm) for the tests consisted of filling the tested composite tubes with concrete. Ready-mixed concrete was used for this purpose. Concrete grade C30 / 37 according to Eurocode 2 [12], with a w/c ratio of 0.52, consistency S3 according to standard [13], maximum aggregate grains 16 mm and exposure classes according to standard [14]: XC3, XD2, XF1, XA1 was ordered. The tubes were fed by blades with concrete which was then successively compacted using a submerged vibrator made by the American company Wacker, model M2000 1.5 kW. During concreting and compaction, the composite tubes were placed vertically on the concrete floor. During compaction, a small amount of water from concrete poured out through the gap between the composite coat of the column and the floor. The applied concrete was tested for compressive strength and Young's modulus. The tests were carried out after 80 to 92 days from concreting using a strength press of the German company Heckert, model DP1600, with a working range from 0 to 1600 kN. The tests on concrete strength were carried out on six concrete cylinders with a diameter of 150 mm and a height of 300 mm, obtaining an average strength f_{cm}=37.1 MPa, with individual results ranging from 32.1 to 38.8 MPa. The mean value of compressive strength obtained experimentally corresponds well with the estimated value of f_{cm}=38.0 MPa recommended for concrete class C30/37 in the standard [12]. The tests on modulus of elasticity were carried out on three concrete cylinders with the same diameters as mentioned before. The obtained mean value of modulus was 31.9 GPa which corresponds well with the estimated value of E_{cm}=32.0 GPa recommended for concrete class C30/37 in the standard [12].

To determine the mechanical parameters of the composite material, sections of tubes (h=200cm) not filled with concrete were prepared. The ends of these tubes were secured on both sides from the inside with concrete stoppers with a height of several centimeters.

Test samples used in the active experiment described here were prepared, examined and stored at a neutral temperature, i.e. at a temperature of about 20° C and ambient humidity around 52%.

During the preparation of CFGFT columns and their components for research, the authors tried to eliminate imperfections. In particular, it concerned the straightness, the shape of cross sections and the axes of the components, as well as their correct execution.

3. Description of tests and observations

The compressive strength of composite and concrete pillars and their coatings was experimentally investigated using a hydraulic strength press manufactured by the Swiss company Walter + Bai AG, model 102/5000-HK4, with a capacity of 5000 kN and a press piston extension from 0 to 100 mm. The load was controlled by displacement, i.e. by the piston stroke of the press. Press equipment enables digital recording of measurement results in the form of discrete signals. The piston stroke measurement was recorded with an accuracy of 0.01 mm, while the measurement of force values was recorded with an accuracy of 0.1 kN. The duration of a single experiment was several tens of minutes, because these were static tests.

All research elements were axially compressed. The support was carried out as articulated on both sides. Shaft joints (Fig. 3a) were used, allowing buckling of columns only in one

predetermined plane. As we know, this way of supporting induces the introduction of boundary conditions (the problem is defined by differential equations) [15].

Before applying the load the specimen were instable. Because of their big mass the composite-concrete specimen had to be installed carefully by the laboratory staff in the load setup. After installing the columns there was no danger in experiments conducting until the columns were possibly buckled too heavily. For the safety reasons, the experiments were finished before achieving 50% loss in compressive force against its maximal value.

The load on samples should be transmitted through the entire cross-section. Therefore, a thick square steel plate with a side length of about 25 cm was placed between the sample tips and the pivot shaft. This was particularly important in the case of compression of concrete and composite pillars. The aim was to transfer the load to the concrete core and reinforced composite coat simultaneously. Additionally, to prevent local damage to the coat by the clamp, the column ends were reinforced with double steel rims from the outside - Fig. 3a.

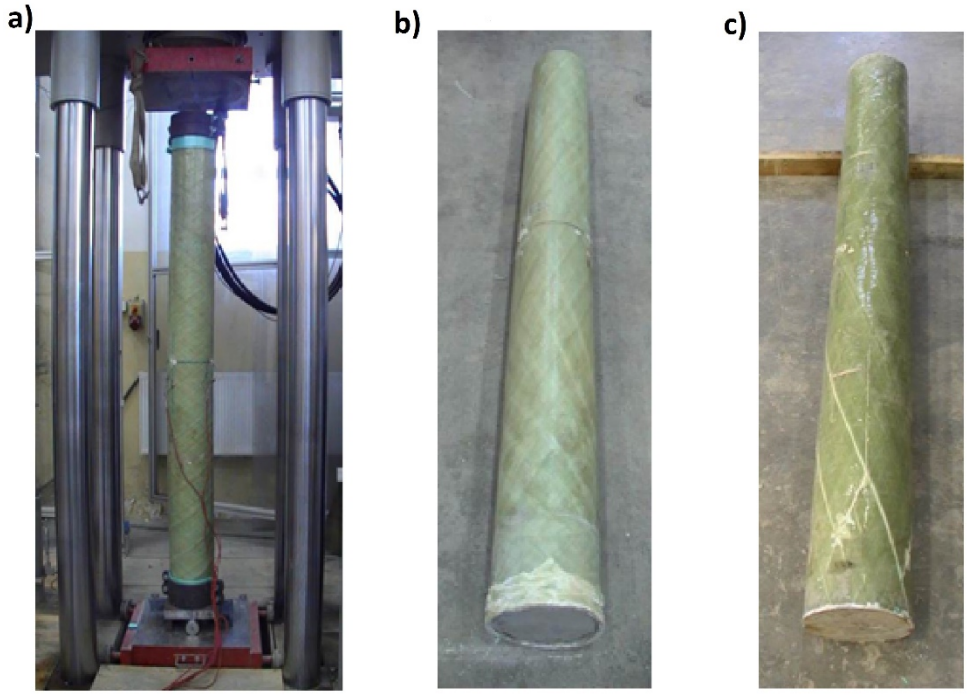

Fig. 3. A sample in the press during the test (a). Research element after destruction: coat with delamination (b), concrete-composite column (c).

Tests of the constructed columns were carried out after about three months from their completion to enable full bonding of the concrete covered with the composite and to minimize the absorption of water (moisture) from the concrete by a polymer composite (based on resins) reinforced with glass fibers. The negative influence of moisture on the strength properties of this type of materials has already been shown in Fig. 1.

Both coating tubes (empty composite pipes) and CFGFT poles underwent compressive static tests in a neutral temperature, i.e. at a temperature of about 20° C and an ambient humidity of about 52%.

During the compression process, in each case a crack appeared in the composite tube, the direction of which was consistent with the direction of the glass fiber winding. The appearance of the crack was always violent - not signaled. After its creation, it was possible to continue loading the member during which the following cracks appeared (Fig. 3c) until the appearance of the so-called destructive crack. These cracks were interfacial defects between glass fibers and polymer matrix. Single glass fibers failures due to compression or tension were not observed. In the case of the coats without concrete core the delamination and stratification phenomena were observed at the column end (Fig. 3b).

4. Results of laboratory tests and their analysis

As a result of the conducted experiments, ordered pairs were obtained: the extension dimension x [mm] of the press piston, the compressive force y [kN] for the jacket as well as the composite-concrete column at different angles of the glass fiber winding. The discrete points $(x_i, y_i), i = 1,2,3, \dots, n$ on the plane correspond to them. Their selected graphical representations are shown in Figs. 4 and 5. Each coordinate is a discrete signal, so it can be analyzed using signal analysis methods.

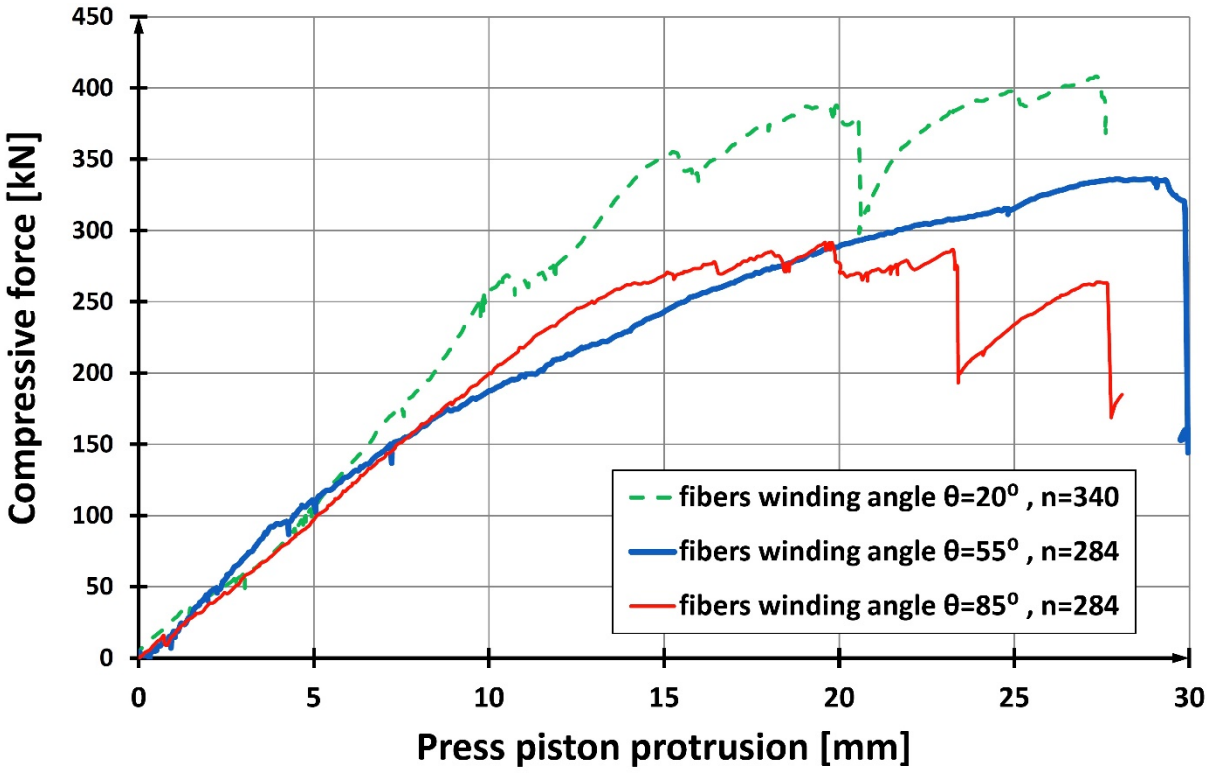

Fig. 4. Graphical interpretation of measurement pairs (x_i, y_i) for the coat by different angles of the glass fibers winding.

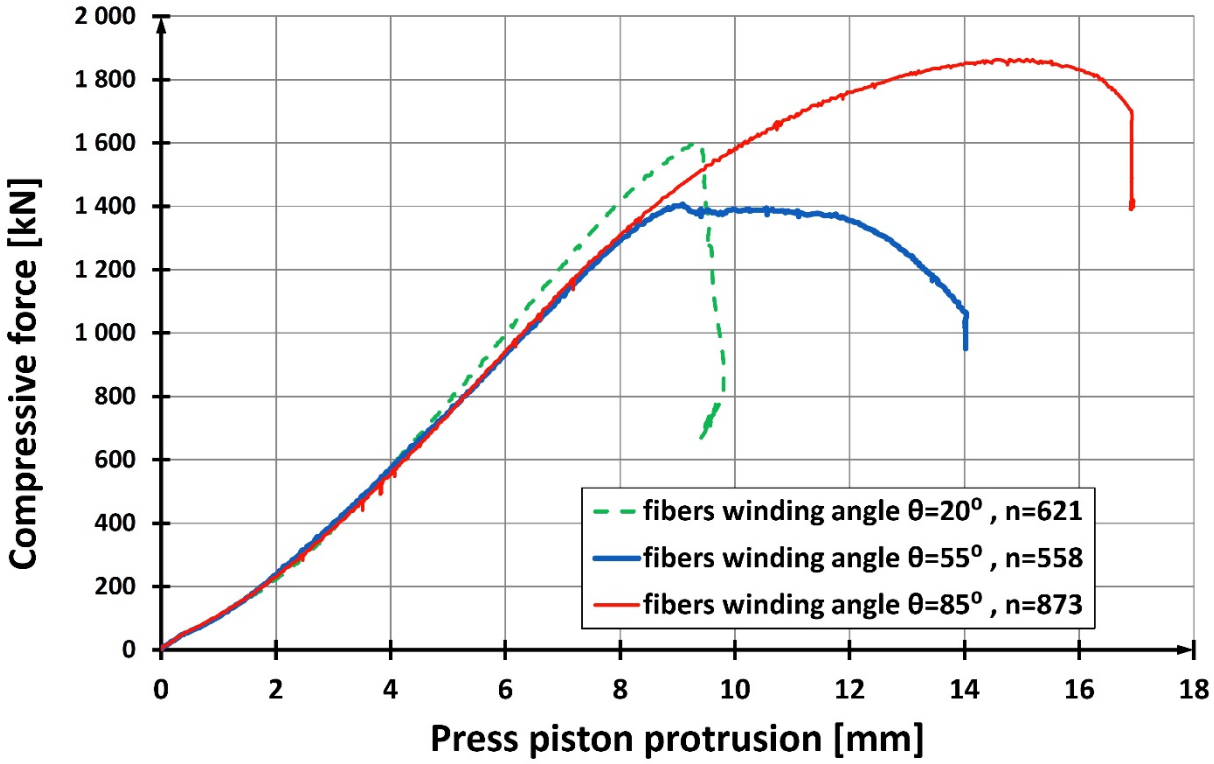

Fig. 5. Graphical interpretation of measurement pairs (x_i, y_i) for a concrete-composite column by different angles of the glass fibers winding.

The load-carrying capacities of the composite-concrete columns are shown in Fig. 5. They totaled 1600 kN, 1406 kN and 1864 kN for the angles of the glass fibers winding 20º, 55º and 85º respectively. A theoretical failure analysis was performed for these three columns under an eccentric compression. An original computer program was used [16]. Second order effects were considered in the program calculations. The mean values of concrete compressive strength and its modulus of elasticity were taken. In additional experimental investigation [16] the following GFRP composite mechanical parameters were determined: compression and tensile strength, compression and tensile moduli of elasticity. All the mentioned parameters were used in the computer calculations. A mathematical model of concrete confined by the composite coating of column was adopted according to [12]. The obtained load-carrying capacities of the columns totaled 1688 kN, 1589 kN and 1807 kN for the angles of the glass fibers winding 20º, 55º and 85º respectively [16].

The obtained graph results (Fig. 4 and Fig. 5) cannot be compared within one group, as well as between representatives of particular groups. The causes are different. For example, for the same piston extension value, there are different values of compressive forces or their absence - Table 3.

Table 3. Fragment of registered discrete measurements.

The size of the piston extension [mm]	Compressive force [kN] Angle of fiber beam		
	20º	55º	85º
0.4	45.9	50.7	52.4
0.4	–	–	53.1
0.41	–	51.8	–
0.46	–	–	57.3
0.5	55.3	–	61.3
0.51	55.5	59.8	–
...	…	…	…
2.43	286.8	302.7	296.2
2.43	–	304.7	297.1

To avoid this situation we can enter a continuous description instead of a discrete description. To describe this, a model should be created and, based on experimental discrete signals, the model should be identified and the optimal model should be chosen from the given class of models by setting $\vec{a}_{opt}$ - Fig.6.

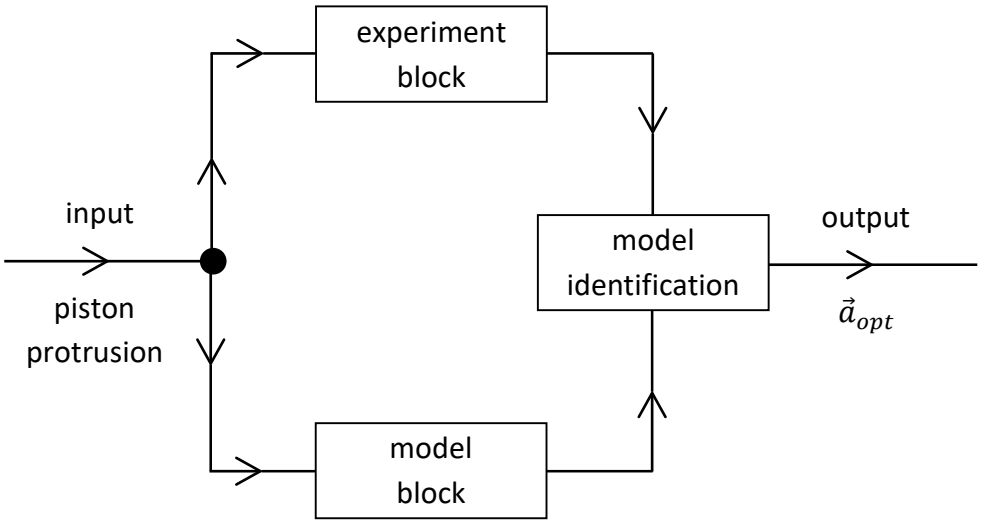

Fig. 6. The control system of the research process: experiment - model.

In the described experiments, general population research was carried out simultaneously due to two features: extension x [mm] of the press piston and the amount of compressive force y [kN] for the coat as well as the composite-concrete column at different angles of the glass fiber winding. In this case, the general population model is a two-dimensional random variable, i.e. a random vector created for each case. We did not stick here to the study of individual variables of the system, but we also tried to examine the relationship between the observed values treated as random variables X and Y respectively, which take measured values of x and y.

The parameter characterizing the relationship between random variables: the stroke X of the press piston and the compressive force Y is the expected value of the product of deviations of

these random variables from their expected values. This parameter is called covariance. It is defined by the following formula:

$$cov(X,Y) = E[(X - EX)(Y - EY)],$$

as long as the expected values EX and EY exist.

Covariance is a value dependent on the measurement units in which the values of random variables X and Y are expressed, i.e. on mm and kN, therefore it is not a good indicator for determining the degree of dependence between random variables X and Y. A dimensionless correlation coefficient $\rho(X,Y) = \frac{cov(X,Y)}{\sigma_X \sigma_Y}$ can be such an indicator, where σ_X , σ_Y are positive variances of random variables X and Y. If our random variables X and Y are independent, then $cov(X,Y) = 0$, and the correlation coefficient determined for them is also equal to zero, i.e. ρ (X, Y) = 0.

Correlation coefficient

$$-1 \leq \rho(X,Y) \leq 1$$

shows how much, on the basis of a two-dimensional random variable, one can conclude that Y is a function of X, i.e. that the value of the piston stroke clearly determines the value of the compressive force.

For all types of glass fiber winding, the correlation coefficient between the random variable determining the piston stroke X and compressive force Y was quite large and amounted to about 0.97 in the case of pole lagging, and about 0.81 in the case of composite - concrete pillars. If so, it is worth looking for a functional dependence between the values measured in the experiment. For this purpose, according to the diagram shown in Figure 6 it was necessary to create appropriate models (classes of models) of dependence for representatives from Figures 4 and 5 of experimental measurements. Their goal is to create equations describing the behavior of the tested compression system, while meeting the conditions essential for its operation, related to the special properties of the compression process of the concrete columns and their coatings, at different angles of the glass fiber winding.

The necessary information about the compression process comes from theoretical considerations, from the analysis of how their postulated mechanisms function in the system and from the conducted experiments illustrating the nature of the response to a specific stimulation by the advancing press piston. It is not analyzed how this mechanism works [17].

From the modeling point of view, the differential equations deserve special attention [15], [17]. Regardless of the differential equations describing the system, there is often a need to formally present other dependencies in the form of algebraic equations dependent on the parameter vector $\vec{a} = [a_0, a_1, a_2, \dots, a_n]$ and compare the obtained results with experimental data in the identification block (in the identification process) - Fig. 6.

Compliance of the model's response with the results of the experiment was expected, and the values of the parameters for which this agreement is the best in the sense of the accepted criterion are the parameters accepted for the model. As a preliminary criterion for accepting the parameter vector $\vec{a}$, the parameters were adopted for which the created function:

$$F = \sum_{i=1}^{n}[y_i - y(\vec{a}, x_i)]^2 \quad (2)$$

will reach the minimum. The following symbols were used: $y(\vec{a}, x_i)$ is the model response for the measured quantities $x_i,\ i = 1, 2, \dots, n$ of the press piston stroke, y_i are the measured compressive forces for the measured values $x_i,\ i = 1, 2, \dots, n$. The values of $\vec{a}$ for which F achieves the minimum, are of course the optimal parameters: $\vec{a}_{opt} = [a_{0opt}, a_{1opt}, a_{2opt}, \dots, a_{nopt}]$. The rest, that is $y_i - y(\vec{a}_{opt}, x_i)$ can be called residuum and denoted by the symbol $res_{\vec{a}_{opt}} y(\vec{a}, x_i)$ i.e. $res_{\vec{a}_{opt}} y(\vec{a}, x_i) = y_i - y(\vec{a}_{opt}, x_i)$.

The following family of functions was adopted in the class of models induced by the parameter vector $\vec{a} = [a_0, a_1, a_2]$:

$$y(\vec{a}, x) = a_2 x^2 + a_1 x + a_0 \quad (3)$$

and for it, model parameters were determined in accordance with formula (2), where the minimum must be determined for the mentioned function. Analysis of the representatives of the experiment results, illustrated in Fig. 4 and Fig. 5, allowed to formulate a preliminary hypothesis about the globally non-linear nature of the relationship: press piston stroke and compressive force, in each of the cases studied, i.e. for composite and concrete pillars, their coatings and various glass fiber winding throughout the entire observation interval. In addition, it was found that the shape of the response differs significantly for individual areas of the independent variable, so using one matching curve will not provide an adequate description of the experimental data. In this case, the use of several functions that locally match the experimental data is justified. It is advisable that individual local functions after joining (gluing) give a smooth description (with a spline function or wavelet [18], [19]). The advantage of this approach, as we shall see further, is a more accurate reproduction of the experimental dependence studied here. Fig. 4 and 5 also clearly show that the functions used to describe the aforementioned dependence must characterize the change in the convex function character in the subinterval. This fact additionally justifies the adopted concept of model solution using the functions described in several formulas. The degree of model fitment was additionally evaluated using the designated components $res_{\vec{a}_{opt}} y(\vec{a}, x_i)$.. The assessment was made using the following quality criteria: (k1) max distance between y_i and $y(\vec{a}_{opt}, x_i)$, $i = 1,2, \dots, n$ in the metric space of the finite sequence, (k2) mean square contingency between y_i and $y(\vec{a}_{opt}, x_i)$, $i = 1,2, \dots, n$, (this figure also corresponds to the corrected by factor $\frac{1}{\sqrt{n}}$ metric (6)), (k3) the average deviation between y_i and $y(\vec{a}_{opt}, x_i)$, $i = 1,2, \dots, n$, which corresponds to the corrected by factor $\frac{1}{n}$ metric (5) and (k4) the slope angle tangent to the curve in radians at selected points The results obtained are shown in Table 4.

Table 4. Representative results of model identification for different families of functions (3) describing relationships between piston stroke quantities and compressive forces in a composite concrete pillar and its coat for different beam angles of glass fibers.

No.	Functional dependence (model (3))	Parameters / evaluation criteria			
		(k1)	(k2)	(k3)	(k4)
A	Pillar buffer/coat				
A1	The angle of the glass fibers winding 20^0				
A1.1	$y = 23{,}71x\ ,\quad x \in < 0{,}10)$	22,74	10,94	8,93	1,53
A1.2	$y = 0{,}82x^2 + 17{,}27x\ ,\quad x \in < 0{,}10)$	10,84	4,49	3,60	1,54
A1.3	$y = -0{,}86x^2 + 40{,}18x - 72{,}06\ ,x \in < 10{,}20)$	15,71	8,11	6,65	1,53
A2	The angle of the glass fibers winding 55^0				
A2.1	$y = 20{,}42x\ ,\quad x \in < 0{,}10)$	16,80	7,26	5,95	1,52
A2.2	$y = -0{,}47x^2 + 23{,}42x\ ,\quad x \in < 0{,}20)$	14,15	4,52	3,86	1,50
A3	The angle of the glass fibers winding 85^0				
A3.1	$y = 19{,}89x\ ,\ x \in < 0{,}10)$	7,01	2,54	2,17	1,52
A3.2	$y = -0{,}99x^2 + 37{,}41x - 71{,}96\ ,\ x \in < 10{,}20)$	10,76	4,11	3,20	1,51
B	Composite - concrete pillar				
B1	The angle of the glass fibers winding 20^0				
B1.1	$y = 15{,}63x^2 + 81{,}48x\ ,\quad x \in < 0{,}4)$	13,01	5,35	4,31	1,57
B1.2	$y = -8{,}81x^2 + 318{,}82x - 587{,}30\ , x \in < 4; 9{,}27)$	26,61	11,34	9,79	1,57
B2	The angle of the glass fibers winding 55^0				
B2.1	$y = 12{,}20x^2 + 95{,}07x\ , x \in < 0{,}4)$	11,87	4,19	3,38	1,57
B2.2	$y = -5{,}53x^2 + 246{,}94x - 342{,}16\ , x \in < 4{,}9)$	46,35	10,15	8,16	1,57
B2.3	$y = 8{,}47x^2 + 106{,}65x\ , x \in < 0{,}6)$	16,89	8,13	6,96	1,57
B3	The angle of the glass fibers winding 85^0				
B3.1	$y = 10{,}03x^2 + 96{,}80x\ , x \in < 0{,}4)$	24,94	6,87	5,15	1,57
B3.2	$y = 10{,}34x^2 + 96{,}25x\ , x \in < 0{,}6)$	27,36	6,27	4,54	1,57
B3.3	$y = -10{,}68x^2 + 334{,}78x - 686{,}54\ , x \in < 6; 8{,}49)$	29,50	6,08	3,96	1,57

Note 1. If (M, d) is a metric space, then metric in this space is also αd , where $\alpha \in R_+$.

Note 2. In the space of finite sequences, the maximum metric is defined by the formula:

$$d(x, y) = \max_{i \in \{1,2,\dots,n\}} |x_i - y_i| \tag{4}$$

It is also possible to define the following metrics in this space:

$$d(x, y) = \sum_{i=1}^{n} |x_i - y_i| \tag{5}$$

$$d(x, y) = \sqrt{\sum_{i=1}^{n} (x_i - y_i)^2} \tag{6}$$

In the formulas (4), (5), (6) the following designations were adopted: $x = \{x_i\}\ , y = \{y_i\}\ , i = 1, 2, \dots, n$.

Note 3. Formula (4) is local, while formula (5) is global.

It is worth noting that the assessment parameters of the model identification process presented in Table 4 are in many cases small, because they constitute about 7 to 9% of the average value of compressive force. These models can be accepted as correctly describing the dependence of the compressive force on the piston stroke for all the cases analyzed here.

From Table 4 it also follows that in some sub-ranges (in the initial part) the dependence can be described by a straight line. Generally, however, this is a curvilinear relationship characterized by a change in the character of the convexity of the function. There is a transition from the convexity down to the convexity upwards especially in the case composite-concrete pillar - Fig.7. It can be clearly seen here that the qualitative nature of the relationship between the measured quantities has been reflected in the model. See and compare with Fig.5.

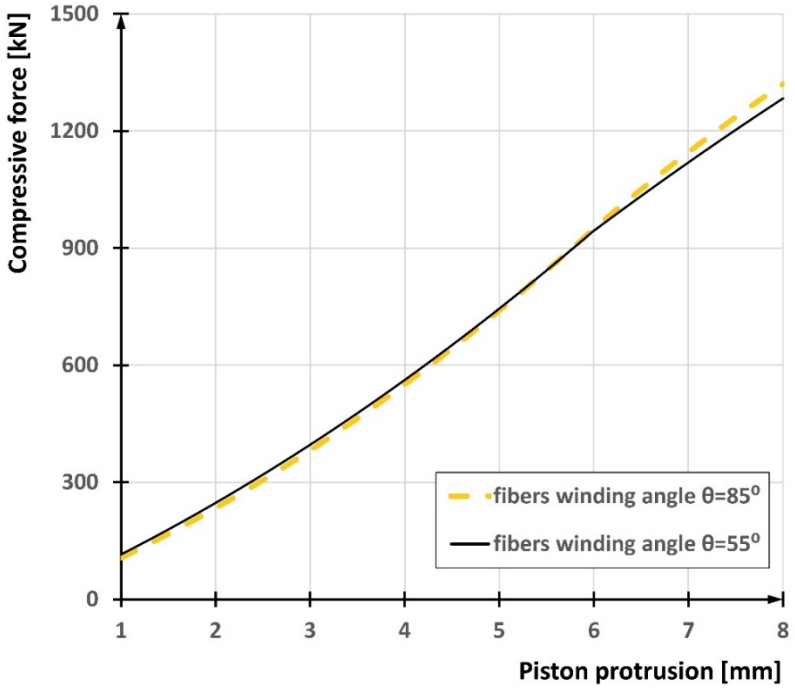

Fig. 7. A fragment of the B2 and B3 diagrams, that is for the composite-concrete pillar (glass fiber winding 55^0 and 85^0)

As it has been mentioned before, the continuous description allows us to compare the values obtained from the model with the values obtained from the experiment for any piston extensions. In addition, the continuous description created allows us to compare compressive forces for different angles of the glass fiber winding corresponding to a given value of the piston extension in the domain. Without a transition to a continuous description, such a task is not feasible. For the comparison of continuous signals, we will use a metric space (M, d) composed of continuous signals defined in the range $< a, b >$. In this space, we define the metric d with the following formula:

$$d(f, g) = \int_a^b |f(x) - g(x)| dx \tag{7}$$

or

$$d(f, g) = \max_{a \le x \le b} |f(x) - g(x)| \tag{8}$$

where $f, g \in M$.

According to Note 1, the metric specified by formula (7) can be corrected with the coefficient $\alpha = \frac{1}{b-a}$.

Note 4. Formula (7) is global, and formula (8) is local in nature, so it allows global or local comparison of results, respectively.

For example, for piston extension from zero to 4 mm, the calculated distances based on formulas (7) and (8) for different fiber windings in the case of a composite concrete pillar are shown in Table 5. They refer to B1.1, B2.1, B3.1 models from Table 4. Table 5 adopts the convention of recording results in the form of a pair: (distance calculated on the basis of formula (7); distance calculated on the basis of formula (8)).

Table 5. Distances between selected curves from Table 4.

	B1.1	B2.1	B3.1
B1.1	(0;0)	(8,89; 13,46)	(8,78; 28,32)
B2.1	(8,89; 13,46)	(0;0)	(8,21; 27,81)
B3.1	(8,78; 28,32)	(8,21; 27,81)	(0;0)

The calculated distances do not differ significantly, but they allow to introduce a partial order between the curves due to the influence of the beam angle of the glass fibers. The ordering relations between the individual curves can be determined by comparing only the first or second elements of the pair. You can also compare whole pairs between themselves, as is the case in partially ordered spaces [17].

Additionally, Fig. 8 presents diagrams of differences between compressive forces for which distances are presented in Table 5. They confirm the observation formulated earlier.

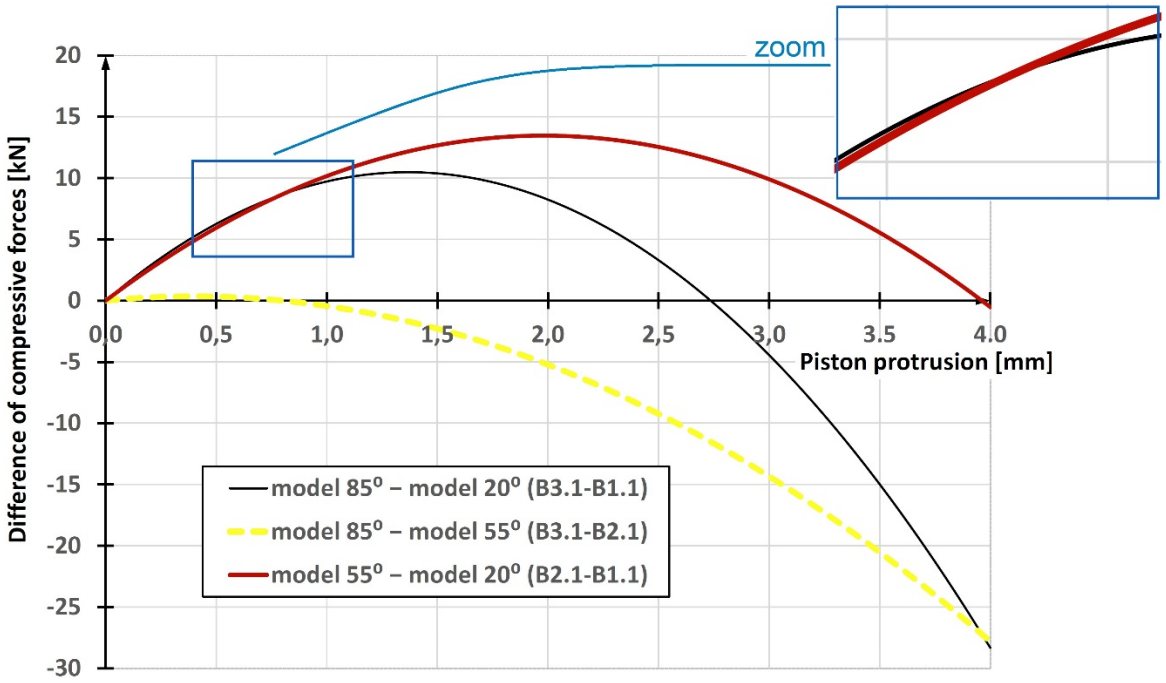

Fig. 8. Diagrams of differences between compressive forces for the composite-concrete columns B in function of the piston protrusion.

For example, intersection of the curves (B3.1 – B1.1) and (B2.1 – B1.1) (red thick and black thin ones) on Fig 8, which are related to the fibers winding angles 85º, 55º and 20º, means, that for the selected piston protrusions the corresponding compressive forces in the concrete-composite columns are equal for the angles 85º and 55º.

5. Conclusions

The correctly set up and carried out active laboratory experiment allowed to perform research on the relationship between the piston extension size and the magnitude of the compressive force. This relationship was registered as representative pairs of discrete signals needed to create a continuous model and to describe the compression of the composite-concrete column and its coating.

Generally, a curvilinear character of the relationship between the size of the piston extension and the magnitude of the compressive force for the composite-concrete column and its coating was found. This curvilinear character takes place especially in the case of a composite concrete column.

The use of several functions defined on the piston extension sub-intervals gave a locally better adjustment of experimental data in the considered class of models. In the case of composite-concrete pillars, at different angles of the glass fiber beam, the models reflected the change in the character of the convexity of the function describing the studied relationships. There is a transition from the convex function down to the convex function up. The use of metric spaces allowed to compare and assess globally and locally models for different angles of the glass fiber beam, as well as to assess the degree of fit of the model and accept the description for further analysis.

The use of partially ordered spaces allows depending on the needs (including practical engineering) to determine the strength relations at different angles of the glass fiber beam for composite-concrete pillars or their coating.

From a theoretical point of view, the behavior of composite-concrete poles can be modeled using beams with a variable cross-section and solved with the use of non-classical operational calculus [20]. This is an innovative approach to the problem which is thereupon difficult to compare with the existing knowledge.

The use of a composite-concrete column coating also prevents physical, chemical and biological degradation of the concrete. In particular, it limits the carbonization of concrete and its cyclical freezing and thawing with penetrating water, thus increasing the lifespan of such pillars.

For damage localization in the coatings of composite-concrete columns wavelet transform [18], [19] or FBG methods can be used in the further research.

In the case of engineering applications, it is worth bearing in mind that composite-concrete pillars, in addition to the previously described properties, are also characterized by high aesthetic values.

Acknowledgement

Scientific research has been carried out as a part of the Project „Innovative recourses and effective methods of safety improvement and durability of buildings and transport infrastructure in the sustainable development" financed by the European Union from the European Fund of Regional Development based on the Operational Program of the Innovative Economy.

Data availability

The raw data as well as the processed data required to reproduce these findings are available to download from:
https://data.mendeley.com/submissions/evise/edit/92zm94vrgw?submission_id=S0263-8223(18)33220-3&token=2b20ba84-9789-4e40-a971-d9c394c5d8ae

References

[1] Quinn JA. Composites – Design Manual. James Quinn Associates Ltd; 2002.

[2] Abdel-Magid B, Lopez-Anido R, Smith G, Trofka S. Flexure creep properties of E-glass reinforced polymers. Composite Structures 2003;62:247–52. doi:10.1016/j.compstruct.2003.09.022.

[3] Li HCH, Herszberg I, Davis CE, Mouritz AP, Galea SC. Health monitoring of marine composite structural joints using fibre optic sensors. Composite Structures 2006;75:321–7. doi:10.1016/j.compstruct.2006.04.054.

[4] Yin WL, Jane KC. Vibration of a delaminated beam–plate relative to buckled states. Journal of Sound and Vibration 1992;156:125–40. doi:10.1016/0022-460X(92)90816-G.

[5] Yan YJ, Yam LH. Detection of delamination damage in composite plates using energy spectrum of structural dynamic responses decomposed by wavelet analysis. Computers & Structures 2004;82:347–58. doi:10.1016/j.compstruc.2003.11.002.

[6] Królikowski W. Reinforced plastics and reinforcing fibers. Warsaw: Wydawnictwo Naukowo-Techniczne; 1988.

[7] Neville AM. Properties of concrete. Pearson Education Limited; 2011.

[8] Abramski M. Load-carrying capacity of axially loaded concrete-filled steel tubular columns made of thin tubes. Archives of Civil and Mechanical Engineering 2018;18:902–13. doi:10.1016/j.acme.2018.01.002.

[9] Chastre C, Silva MAG. Monotonic axial behavior and modelling of RC circular columns confined with CFRP. Engineering Structures 2010;32:2268–77. doi:10.1016/j.engstruct.2010.04.001.

[10] ASTM D2584-11: Standard Test Method for Ignition Loss of Cured Reinforced Resins

2011.

[11] Ochelski S. Experimental methods of mechanics of structural composites. Warsaw, Poland: Wydawnictwa Naukowo-Techniczne; 2004.

[12] EN 1992-1-1:2004. Eurocode 2: Design of concrete structures - Part 1-1: General rules and rules for buildings 2004.

[13] EN 12350-2: 2009. Testing fresh concrete - Part 2: Slump-test 2009.

[14] EN 206:2013+A1:2016. Concrete – Part 1: Specification, performance, production and conformity. 2016.

[15] Mieloszyk E. Application of non-classical operational calculus to solving some boundary value problem. Integral Transforms and Special Functions 1998;9:287–92. doi:10.1080/10652460008819262.

[16] Abramski M. Short-time load-carrying capacity of concrete-filled FRP circular tube columns. Experiments, theory, calculation. Gdansk: Gdansk University of Technology; 2019.

[17] Mieloszyk E. Non-classical operational calculus in application to generalized dynamical systems (in Polish). Gdansk: Polish Academy of Sciences Scientific Publishers; 2008.

[18] Li H, Yi T, Gu M, Huo L. Evaluation of earthquake-induced structural damages by wavelet transform. Progress in Natural Science 2009;19:461–70. doi:10.1016/j.pnsc.2008.09.002.

[19] Yi TH, Li HN, Sun HM. Multi-stage structural damage diagnosis method based on ‘energy-damage’ theory. Smart Structures and Systems 2013;12:345–61. doi:10.12989/sss.2013.12.3-4.345.

[20] Milewska A. A solution of non-linear differential problem with application to selected geotechnical problems. Archives of Civil Engineering 2011;57:187–97. doi:10.2478/v.10169-011-0014-4.